JOURNAL OF MATERIALS SCIENCE 20 (1985) 1602–1615

Solution crystallization of polyethylene at high temperatures

Part 3 *The fold lengths*

S. J. ORGAN, A. KELLER
H. H. Wills Physics Laboratory, University of Bristol, Tyndall Avenue, Bristol, UK

Single crystals of polyethylene have been grown from solution in various solvents at temperatures between 70 and 120° C. This represents an overlap in crystallization conditions with those used for melt growth, where substantial isothermal thickening is known to occur during growth. The crystal thicknesses have been measured by Raman spectroscopy. Values of the equilibrium dissolution temperature and fold surface free energy are calculated for each solvent and the results analysed using the kinetic theory. Variations in crystal properties with time of crystallization are also investigated. A specific dependence of fold length on supercooling has been found to apply over the whole temperature range, consistent with predictions by the kinetic theories of crystallization in spite of changes in morphology which are incompatible with assumptions underlying the theoretical model. No evidence for isothermal thickening has been observed, except possibly for a small marginal effect at the highest temperature of 120° C investigated, over the same temperature range where melt crystallized material shows the effect prominently. Crystals grown at all temperatures displayed a rise in dissolution temperature with time which could be associated with an increase in surface perfection. All these findings have wider implications for our picture of polymer crystallization and crystal structure which are discussed here. A further, explicit, correlation with melt crystallization is deferred to a subsequent publication.

1. Introduction

This paper is the third in a series of three which investigate various properties of single crystals of polyethylene grown from solution at temperatures up to 120° C. The motivation behind the work is outlined in the introduction of Part 1 [1]. Briefly, an overlap has been achieved in the crystallization conditions used for melt and solution growth, both in terms of absolute crystallization temperature (T_c) and supercooling (ΔT). This enables direct comparisons to be made between the two processes and provides the basis for a re-evaluation of the available crystallization theories. The experimental techniques and results relating to the melt case are documented elsewhere [2–4] and will be raised again in the two papers following the present series [5, 6] as outlined in the introduction of Part 1 [1]. In this series we consider various relevant aspects of the complimentary single crystal studies.

Part 1 of the series [1] was concerned with two-dimensional crystal habits. As the crystallization temperature is raised crystals become more elongated in the b direction and their faces become curved, showing increasing deviation from the exact crystallographic faces obtained at lower temperatures. These changes, which reflect trends seen under similar conditions in the melt, are documented and discussed.

Part 2 [7] goes on to examine the three-dimensional structure and internal sectorization of the crystals using dark-field electron microscopy, paraffin decoration and melting studies. A gradual decrease in distinction between different sectors of crystals is detected as they become more elongated.

0022–2461/85 $03.00 + .12

In this paper, Part 3, the fold lengths of the same crystals are determined using Raman spectroscopy. Crystal thicknesses, or fold lengths, are of fundamental importance to the issue of polymer crystallization. Early measurements of crystal thicknesses [8] revealed a dependence of the form

$$l \approx C_1/\Delta T + C_2 \quad (1)$$

where l is the thickness, C_1 and C_2 are constants and ΔT is the supercooling. This led to the formulation of the kinetic theory, which in a more developed form [9] remains the most successful theory of polymer crystallization.

Under normal conditions, single crystals formed isothermally are assumed to grow with a constant fold length (although this is disputed by some [10]). However, if heated subsequently to a higher temperature, the crystals will thicken by an amount dependent on both the temperature and the time of annealing [11]. In the case of melt growth, which normally takes place at temperatures much higher than those used for solution crystallization, an additional thickening effect is seen, known as isothermal annealing [12, 13]. In this case crystals thicken during growth, so that the measured fold length of a melt crystallized sample is not that with which it formed, but larger by an amount dependent on the time of crystallization. A recent development of a technique previously used by Cormia *et al.* [14] has enabled melt crystallization to be performed at much higher supercoolings than was previously possible. Here the effect of isothermal thickening is greatly reduced and values can be obtained for the initial thickness of the lamellae [3]. At the lowest temperatures ($\sim 85^\circ$ C) no thickening was detected even after prolonged storage at T_c. If isothermal thickening can be prevented by lowering the crystallization temperature in the melt, can it be induced by raising T_c in solution? Most of the crystals described in Parts 1 and 2 [1, 7] were grown at temperatures where isothermal thickening would occur in the melt, and where single crystals annealed in the form of dried sedimented mats would undergo substantial thickening. Measurements of the fold lengths of these crystals are of fundamental importance for several reasons:

1. For testing the applicability of the kinetic theory over an extended range of growth conditions.

2. To investigate the possiblity of isothermal thickening during solution crystallization at high temperatures.

3. To investigate possible origins of the unusual curved morphologies exhibited by these crystals.

The work presented here is divided into two sections. First, the fold lengths and dissolution temperatures of the crystals described in Part 1 [1] were measured. The results were analysed using the kinetic theory and examined for any evidence of isothermal thickening. A similar study has been carried out by Nakajima *et al.* [15, 16], who measured, using X-rays, the thicknesses of crystals grown from various solvents at temperatures up to 109° C. However, in that case the corresponding crystal morphologies were not studied and the possibility of isothermal thickening was not considered. Secondly, a series of ageing experiments were performed in which crystal properties were examined as a function of crystallization time in an attempt to quantify any changes which might occur during crystallization. The fold lengths and dissolution temperatures were measured and gold decoration used to reveal differences in surface perfection. Gold decoration shows up details of surface structure by revealing differences in gold nucleation density both within and between different crystal surfaces [17]. These differences in nucleation density were found to arise from residual solvent [18], which is retained to different extents by different crystal surfaces. The effect can be accentuated by flooding the decorated crystals with a swelling agent, which allows loose elements on the surface to mobilize and cluster together. Thus surfaces with a higher proportion of long cilia and loose loops will be more coarsely decorated, and differences in gold nucleation density can be directly correlated with differences in surface perfection.

Previous ageing experiments of this kind [19, 20] have involved crystallization at relatively low temperatures: 85 and 90° C. Neither Mandelkern [19] nor Weaver and Harrison [20] found any increase in crystal thickness with crystallization time. Mandelkern also measured the crystal dissolution temperatures and found them to be invariant. Weaver and Harrison found no change in melting temperatures but did detect a possible small increase in the heat of fusion with increased crystallization time, and found a considerable difference in the swelling behaviour of the crystals. Variations in swelling behaviour have been studied extensively by Udagawa and Keller [21]. They found that the amount of swelling is reduced by

heat treatment, even at temperatures too low to produce a fold-length increase. Weaver and Harrison [20] obtained a similar result in their ageing experiment, where the amount of swelling decreased markedly with the time the crystals were held at the crystallization temperature, even though the crystal thickness did not change. In the work presented here higher crystallization temperatures, where isothermal thickening might reasonably be expected to occur, are used.

Fold lengths were measured by Raman spectroscopy using the relationship derived by Fraser [22]:

$$l_R = \frac{316.9}{\Delta\nu} \quad (2)$$

where l_R is the Raman fold length in nm and $\Delta\nu$ is the frequency of the longitudinal acoustic mode (LAM) vibration. The frequency distribution can be converted to a fold length distribution by multiplying the intensity at frequency ν by a factor $K_\nu\nu^2$ after a suitable background has been subtracted [23]. These corrections can have a substantial effect on the peak position for the lowest frequency vibrations, particularly where the half-width of a peak is large [24]. For solution grown single crystals, where the vibrational frequencies are relatively high and the peaks are well-defined, the corrections do not significantly affect the results and are not generally applied. l_R is calculated directly from the peak position in the frequency distribution.

Equilibrium dissolution temperatures, T_d^0, were found for each solvent by extrapolation, using the relationship

$$T_d = T_d^0 - \frac{2T_m^0\sigma_e}{l\Delta H} \quad (3)$$

Here T_d is the dissolution temperature of a crystal of fold length l (assumed equal to l_R). T_m^0 is the equilibrium melting point of the polymer, σ_e the fold surface free energy and ΔH the heat of fusion. Other commonly used methods are the visual determination of dissolution temperatures of high-pressure crystallized polyethylene with nearly fully extended chains [25] and extrapolation of T_d against T_c curves to the point where $T_d = T_c$ [26]. T_d^0 values obtained using Equation 3 are comparable with those obtained from extended chain crystals. Values deduced from T_d against T_c extrapolations tend to be somewhat lower.

2. l_R against T_c Measurements

2.1. Experimental details

All the crystals were grown isothermally from self-seeded 0.05% w/v solutions of pre-fractionated Rigidex 50, as described in Part 1 [1]. The solvents used were xylene, octane, dodecane, hexadecane, tetracosane, hexatriacontane, hexyl acetate, ethyl esters from ethyl caproate ($CH_3(CH_2)_4CO_2C_2H_5$) to ethyl laurate ($CH_3(CH_2)_{10}CO_2C_2H_5$) and the aliphatic alcohols dodecanol and tetradecanol.

2.1.1. Measurements of the Raman fold lengths

Samples were prepared for Raman spectroscopy by filtering the crystal suspension, washing thoroughly, then drying under vacuum to remove residual solvent. The resultant powder, consisting of randomly oriented single crystal aggregates, was put into either a glass capillary tube sealed at one end or a spinning-cell apparatus. The spinning-cell spreads the area of illumination by continuously rotating the sample in the beam, thus reducing the risk of burning. Raman spectra were obtained using a Coderg T800 triple monochromator spectrometer. In order to resolve the LAM peaks, which occur very close to the exciting line, small slit widths, typically 150 to 200 nm, were used. The light source was a CRL model 52 argon ion laser operating at 514.5 nm (green) set to give a power of approximately 200 mW at the sample. The scattered light was collected at 90° to the incoming laser beam and analysed using an Ortec/Brookdeal 5CI photon counting system interfaced with an Apple II + microcomputer. The exciting line was recorded onto the spectrum, using a metal barrier to protect the photon counter from the full intensity of the laser. This enables precise calculation of wavenumber shifts. The spectrum was scanned over typically 40 cm^{-1} at a rate of 1/8 cm^{-1} sec^{-1}. Data were sampled every second and a 25-point smoothing routine applied. Peak positions were found after a suitable background had been subtracted, and converted to fold lengths using the relationship given in Equation 2.

2.1.2. Measurement of dissolution temperatures

Dissolution temperatures were measured using a Perkin-Elmer DSC-2 differential scanning calorimeter. Approximately 0.1 mg of crystals, in suspension in their original solvent, were heated in a hermetically-sealed volatile sample pan. A heating

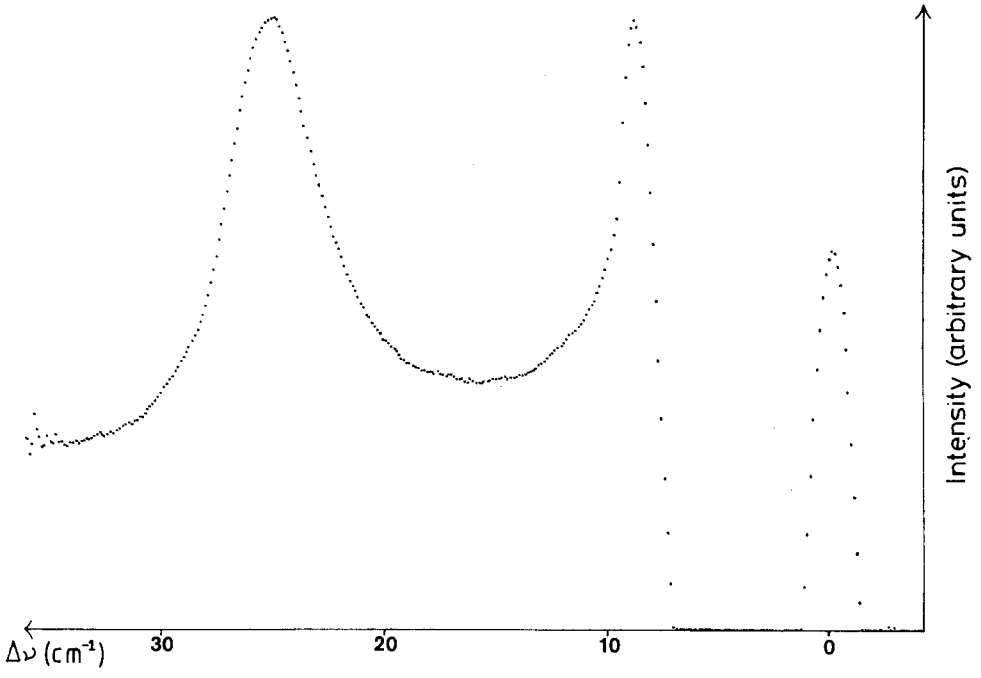

Figure 1 Raman spectrum of crystals grown from octane at 89.4° C.

rate of 5° C min^{-1} was used. Fast heating rates cause superheating of the sample and give anomolously high values of T_d, whilst slow heating rates have the complication that some crystals may thicken during heating. At 5° C min^{-1} the degree of superheating is small. Preliminary experiments were carried out to estimate its magnitude, and results were corrected for the effect. No appreciable thickening occurs using this heating rate. T_d values quoted correspond to the peak position of the dissolution endotherm, calibrated using an Indium standard, and corrected for superheating. T_d^0 values were obtained by extrapolation using Equation 3.

2.2. Results

2.2.1. Crystal fold lengths

Crystals grown from xylene, octane, dodecane, hexadecane, hexyl acetate, ethyl esters and dodecanol all produced well-defined peaks in their low frequency Raman spectra. A typical spectrum is shown in Fig. 1. The calculated fold lengths are shown in Fig. 2 as a function of crystallization

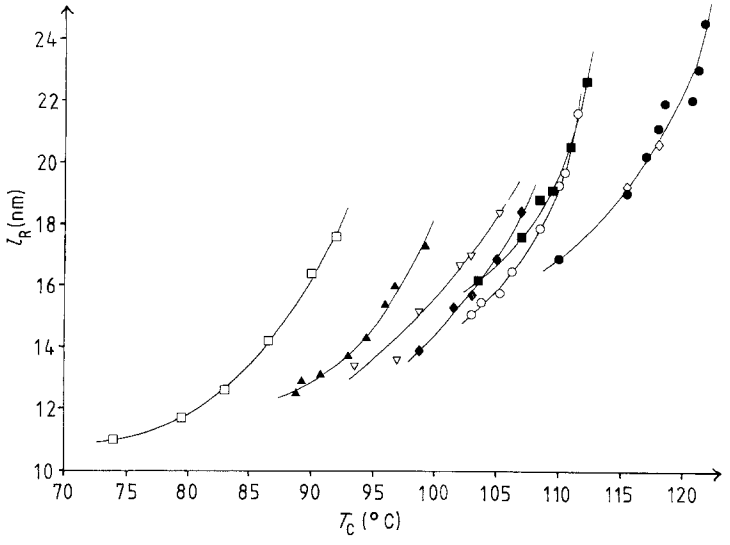

Figure 2 Raman fold lengths, l_R, as a function of crystallization temperature, T_c. □-xylene, ▲-octane, ▽-dodecane, ♦-hexadecane, ○-ethyl esters, ■-hexyl acetate, ◇-tetradecanol, ●-dodecanol.

temperature. Some crystals grown from tetradecanol showed a tendency to burn, but in cases where a clear Raman signal could be obtained the results agreed well with those obtained from crystals grown in dodecanol. Burning was also a problem in the case of crystals grown from tetracosane and hexatriacontane, probably due to residual solvent in the samples, and reliable results could not be obtained for these samples. The Raman peaks become more difficult to resolve as they approach the frequency of the exciting line. The fold length results presented in Fig. 2 are subject to an error ranging from ± 0.2 nm at the lowest crystallization temperatures to ± 0.8 nm at the highest values. A frequency correction has not been applied. The correction has a negligible effect at the higher frequencies, and at lower values depends on a rather arbitrary background subtraction. In an extreme case, the peak position could be shifted by up to about 0.5 cm^{-1}, which would decrease the calculated fold length by about 0.7 nm. This is within the quoted error range. Crystallization temperatures are accurate to within ± 0.2° C. The plot of l_R against T_c for crystals grown from the different solvents gives a series of smooth curves. These curves are of similar shape, approximately displaced from each other along the temperature axis.

Attempts were made to measure the thicknesses of crystals grown from tetracosane and hexatriacontane by measuring shadow lengths on electron micrographs. The results were inconclusive, showing considerable deviation within some samples and a lack of correlation between samples. This is rather surprising since both the morphology (see Part 1) and the dissolution temperature (see next section) behave quite regularly. Both these solvents are fairly long chain hydrocarbons, with a structure very similar to that of polyethylene. It seems plausible that some hydrocarbon chains may be partially incorporated into the crystal structure during crystallization, leaving loose ends which would contribute to a disordered surface layer. Solvent molecules could also become entangled in the crystal surface and be unable to escape due to their large size. A layer of solvent molecules attached to the crystal surface in some way could account for the anomolously high crystal thicknesses and the wide variation in values. It could also explain why Raman signals could not be obtained, even after prolonged washing of the crystals. Variations in the thickness of the layer between samples could be due to slight variations in the washing procedure and to the subsequent time the crystals were left to stand in suspension in xylene. Crystals grown from tetracosane and hexatriacontane are omitted from subsequent analyses.

2.2.2. T_d^0 and σ_e values

Fig. 3 Shows crystal dissolution temperatures plotted as a function of reciprocal fold length, using the l_R values shown in Fig. 2. Errors are in the range 0.2 to 0.3° C for T_d and 0.1 to 0.2 × 10^{-2} for $1/l_R$, too small to show clearly on the graph. The points lie on a fairly good straight line for each solvent. Best fit lines have been calculated

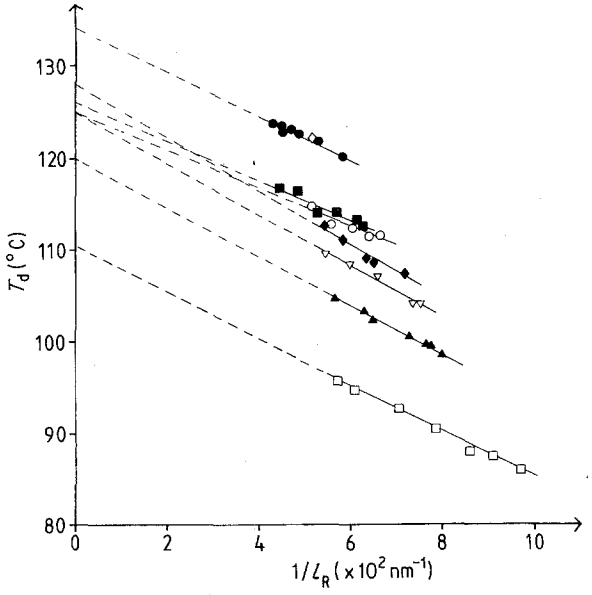

Figure 3 Crystal dissolution temperatures, T_d as a function of reciprocal fold length, $1/l_R$. □-xylene, ▲-octane, ▽-dodecane, ♦-hexadecane, ○-ethyl esters, ■-hexyl acetate, ◇-tetradecanol, ●-dodecanol.

TABLE I Calculated values of equilibrium dissolution temperatures, T_d^0 and surface free energies σ_e, for crystals grown from various solvents

Solvent	T_d^0 (° C)	σ_e (erg cm^{-2})
Xylene	110.5 ± 1.0	82.2 ± 3.3
Octane	120.2 ± 1.4	89.8 ± 6.3
Dodecane	125.0 ± 1.6	93.8 ± 7.5
Hexadecane	128.1 ± 1.6	98.9 ± 9.9
Ethyl esters	125.1 ± 1.8	69.5 ± 10.4
Hexyl acetate	126.2 ± 1.4	72.1 ± 7.2
Dodecanol	133.6 ± 2.0	75.8 ± 13.6

and extrapolated back to $1/l_R = 0$ to give a value for T_d^0. The results are listed in Table I. σ_e values were calculated from the gradients of the lines using a value of $\Delta H = 2.8 \times 10^9$ erg cm^{-3}, and these are also given in Table I. The error margins quoted for T_d^0 and σ_e are based on estimations of the lines of maximum and minimum probable gradient through the points. The linearity of the points justifies the assumption that the quantity $\sigma_e/\Delta H$ does not vary greatly with temperature. σ_e values are of similar magnitude in all cases, but are generally higher for the paraffinic solvents. Both σ_e and T_d^0 show a gradual increase with length of chain within the paraffin series.

Fig. 4 shows the dissolution temperatures of crystals grown from tetracosane and hexatriacontane as a function of crystallization temperature. In contrast to the shadow length results, the dissolution temperatures show a regular increase with T_c. Extrapolation to the point where $T_d = T_c$ yields values of $T_d^0 = 120.6 \pm 0.6$° C for crystals grown in tetracosane and $T_d^0 = 121.6 \pm 1.0$° C for those grown in hexatriacontane. As mentioned previously this method of calculation of T_d^0 tends to yield lower values than other methods, and is not considered to be reliable. For comparison, T_d^0 values obtained in this way are 112.4 ± 2.0° C for octane, 113.6 ± 1.4° C for dodecane and 119.0 ± 2.5° C for hexadecane (compared to 120.2, 125.0 and 128.1° C respectively, from Table I). Thus when the same method of calculation is used, tetracosane and hextriacontane follow the same trend as shown by the other paraffinic solvents, i.e. T_d^0 increases with increasing chain length, to approach the value found in the melt. The values given above were not used in calculating supercoolings for comparative purposes.

2.2.3. *Variation of fold length with supercooling*

Fig. 5 shows the Raman fold lengths of the crystals, l_R, plotted against supercooling, ΔT, where $\Delta T = T_d^0 - T_c$. Representative error bars for each solvent are shown on the graph; horizontal error bars give the possible shift of the curve as a whole for each solvent, while vertical error bars refer to individual

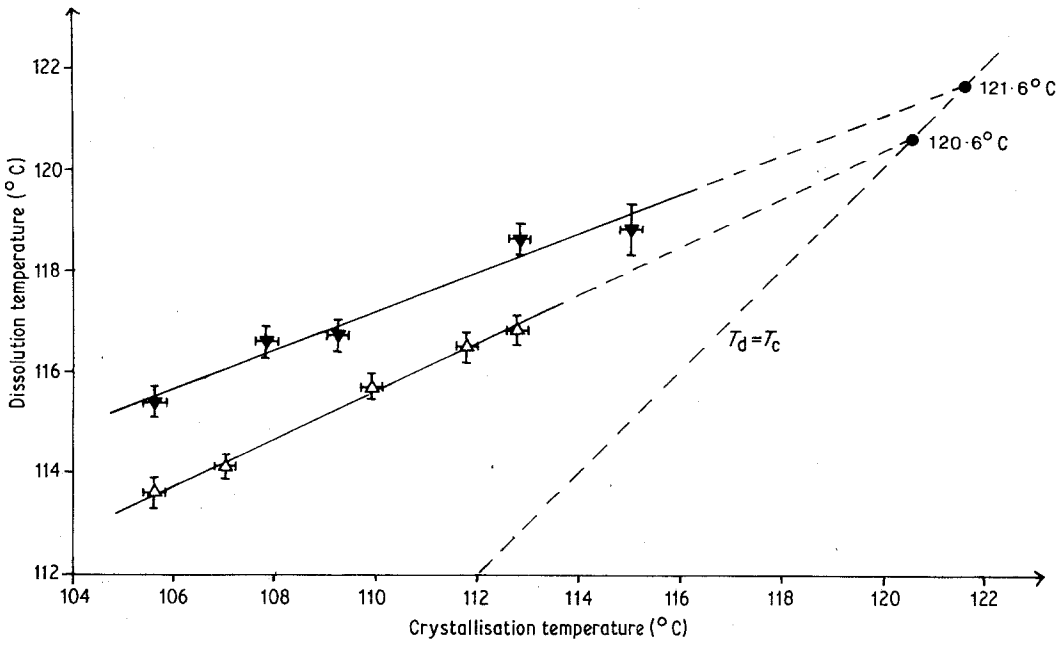

Figure 4 Dissolution temperatures of crystals grown from tetracosane (△) and hexatriacontane (▼) as a function of crystallization temperature, showing extrapolations to the points where the two are equal.

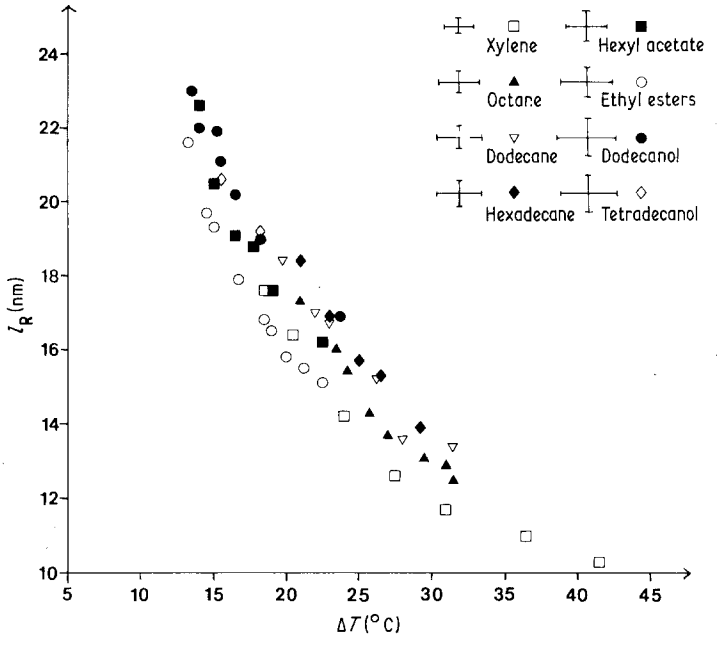

Figure 5 Variation of Raman fold length, l_R, with supercooling, ΔT.

points. There is some dispersion among the points, and shifting curves along the supercooling axis cannot bring all the points to lie on exactly the same curve. However, the overall trend is one of dependence of fold length on supercooling, with some small variations due to solvent. At high supercoolings the curve appears to be tending towards a constant fold length, but this is outside the range of the present experiment. As the supercooling is reduced, the fold length increases more and more rapidly, in accordance with the predictions of kinetic theories.

3. Ageing experiments

3.1. Experimental procedures

Most crystals were prepared using the methods described in Part 1 [1]. The initial crystal suspension was divided into several portions, which were put into identical crystallization vessels and subjected to the same self-seeding procedure. The portions were then transferred simultaneously to an isothermal crystallization bath and left for varying lengths of time, t_c, to crystallize. Each sample was filtered at the crystallization temperature after the appropriate time, then quenched with solvent at room temperature as described previously.

Crystals of Rigidex 50 with the lowest molecular weights removed (see Part 1) were grown under the following conditions:

Experiment I–from 0.05% solution in xylene at 86.0° C.

Experiment II–from 0.05% solution in hexyl acetate at 108.5° C.

Experiment III–from 0.05% solution in dodecanol at 118.0° C.

Experiment IV–from 0.05% solution in dodecanol at 120.0° C.

Experiment V–from 0.05% solution in dodecanol at 120.4° C, using the modified apparatus shown in Fig. 6.

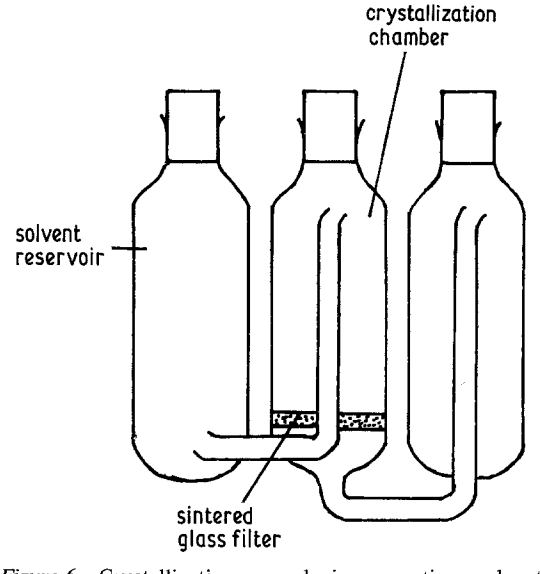

Figure 6 Crystallization vessel incorporating solvent reservoir.

The vessel shown in Fig. 6 incorporates a reservoir containing fresh solvent at the crystallization temperature, allowing for isothermal filtration and re-suspension of the crystals during crystallization. After two hours, when the bulk of the material could be seen to have crystallized, the crystal suspension was filtered to remove any low molecular weight material remaining in solution, and fresh solvent was added from the reservoir. About half the resultant suspension was removed, washed thoroughly with warm xylene (50 to 60° C) to remove the original solvent, sedimented into a mat and dried thoroughly. Samples of this mat were sealed in DSC pans and placed in the crystallization bath along with the remaining crystal suspension. Further portions of the suspension were removed after extra storage times of 3.0, 20.0, 98.0 and 332.0 h. Samples of the crystal mat were removed after annealing for the same intervals of time.

Each series of crystals were prepared for DSC and Raman spectroscopy as described previously. The Raman fold lengths of all the crystals were measured in the manner described above. Most results are uncorrected, apart from an appropriate background subtraction, but the frequency correction due to Snyder and Scherer [24] has been applied to the results of Experiment V.

Dissolution temperatures of the crystals from Experiments I–V were measured as described previously. All values represent extrapolations to zero heating rate.

Crystals from Experiment I were decorated by vacuum evaporation of a thin film of gold and examined in the electron microscope. The morphology of the other crystal preparations was examined by phase contrast optical microscopy and TEM.

3.2. Results

In examining the properties of the crystals grown in Experiments I–V, different investigative techniques have been given priority for the various cases, in order to highlight different aspects of the crystallization process. The results from Experiments I and II are presented first, and here the main emphasis is on changes in the crystal surface during crystallization. Results from Experiments III and IV concentrate more on the fold lengths, and Experiment V is an extension of IV, incorporating several additional features.

3.2.1. Experiments I and II

The Raman fold lengths of crystals from Experiments I($T_c = 86.0°$ C in xylene) and II($T_c = 108.5°$ C in hexyl acetate) were constant, within experimental accuracy, for all crystallization times. The values obtained were 14.5 ± 0.3 and 18.8 ± 0.4 nm, respectively.

The dissolution temperatures, however, showed a slight increase with increasing crystallization time in both cases. These results are shown in Fig. 7, using a logarithmic time scale for convenience. The increase in T_d with crystallization time is small but systematic, and suggests some time dependent change in structure. From Equation 3, differences in dissolution temperature are most likely to arise from variations in the value of the term $\sigma_e/l\Delta H$. Since no thickening is detected, either an increase in ΔH or a reduction in σ_e is implied. An increase in the degree of crystal perfection would be reflected in a sharpening of the dissolution endotherms, but no such effect was seen. Changes in σ_e might be reflected by a difference in surface structure, and indeed gold decoration of crystals from Experiment I did reveal a change in the surface nucleation density with time. Figs. 8a and b show crystals from similar preparations grown at 72.0° C with $t_c = 2$ and 170 h respectively, which were simultaneously decorated with gold. The decoration was noticeably coarser on the surfaces of the crystals with the shorter crystallization time. The effect was accentuated by flooding the decorated crystals with xylene, as shown in Figs. 8c and d. The change in nucleation density with time implies that the proportion of long cilia and loose loops on the crystal surface is decreasing as the time of crystallization is extended. This reorganization presumably lowers the fold surface free energy, causing the observed rise in dissolution temperature, but leaves the fold length unchanged. The results are consistent with the changes in swelling behaviour reported previously [20, 21].

3.2.2. Experiments III and IV

The dissolution temperatures of crystals from Experiments III ($T_c = 118.0°$ C in dodecanol) and IV ($T_c = 120.0°$ C in dodecanol) are shown in Fig. 9a. Again a gradual increase in dissolution temperature with crystallization time is seen, and this is more pronounced for the crystals grown at the higher temperature.

The corresponding Raman fold lengths are shown in Fig. 9b (the point corresponding to $t_c =$

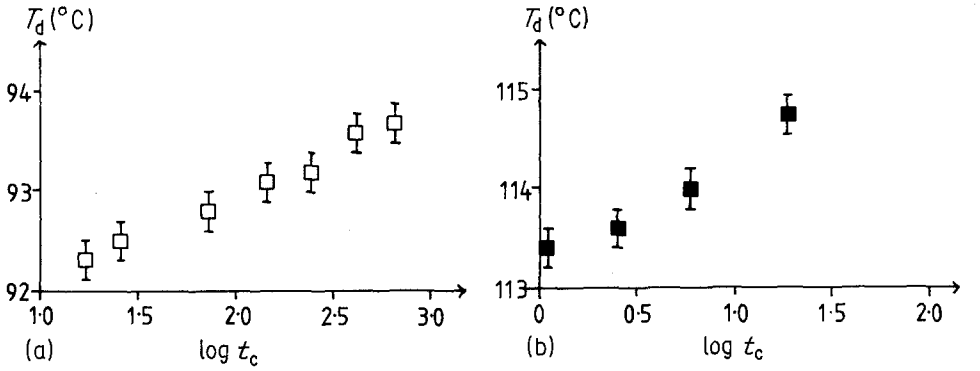

Figure 7 Dissolution temperatures, T_d, as a function of crystallization time, t_c. (a) Crystals grown from xylene at 86.0° C (b) Crystals grown from hexyl acetate at 108.5° C.

1.5 h in Experiment IV is omitted since no clear Raman signal could be obtained). Within the accuracy of measurement, there is no change in fold length with crystallization time for the crystals grown at 118.0° C. However, for the crystals grown at 120.0° C, some thickening is indicated. Due to the close proximity of the LAM peaks to the exciting line and also to a gradual broadening of the peaks with crystallization time, the accuracy of the results is rather lower in this case. The rate of thickening suggested by the data is approximately 1.8 nm per decade of hours.

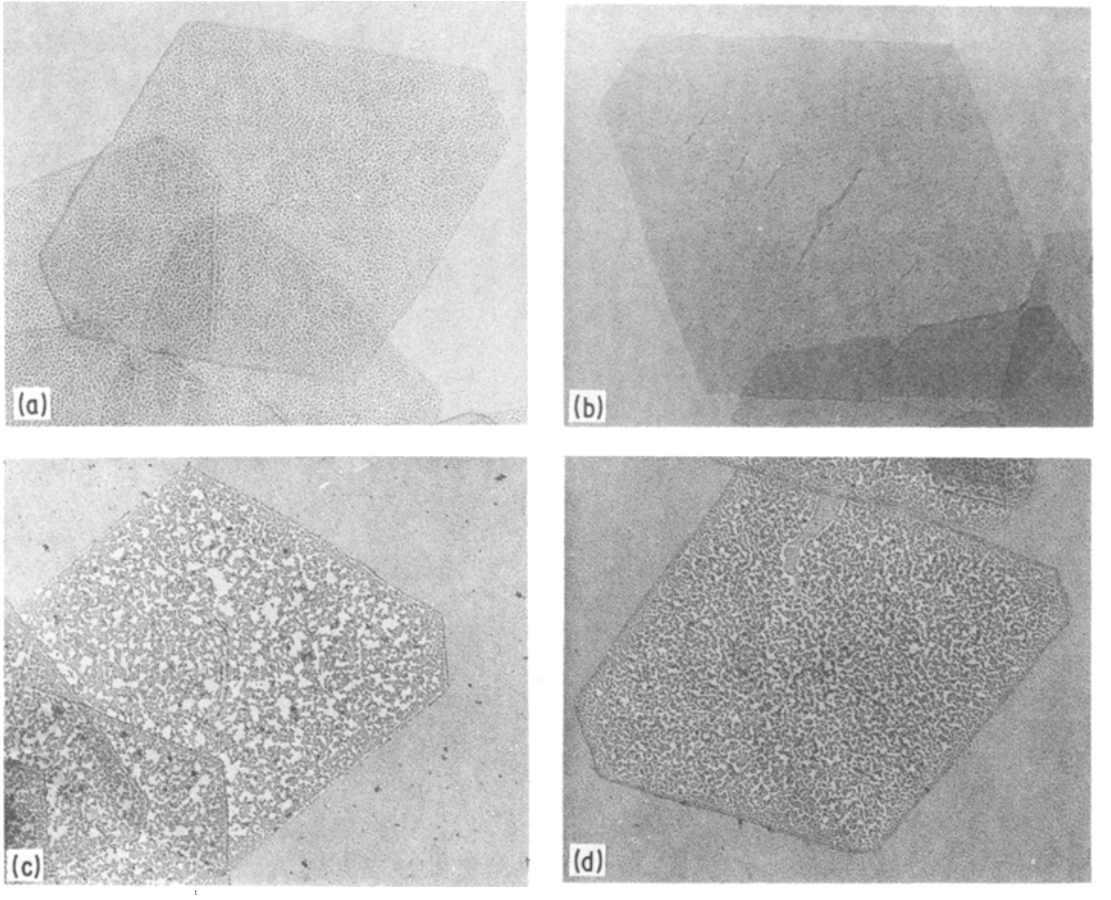

Figure 8 Crystals grown from xylene at 72.0° C. (a) and (c) t_c = 2 h. (b) and (d) t_c = 170 h. All the crystals are gold decorated, (c) and (d) were flooded with xylene subsequent to decoration (All approximately × 30 K).

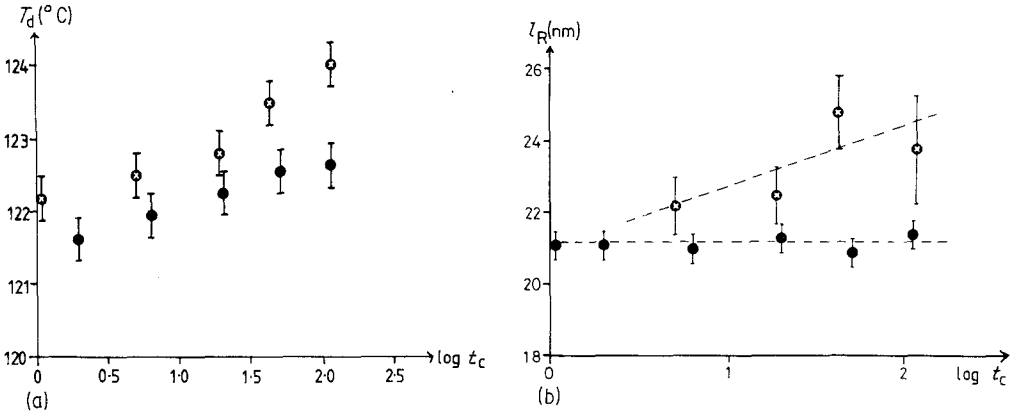

Figure 9 (a) Variation of dissolution temperature, T_d with crystallization time, t_c. (b) Variation of Raman fold length, l_R, with crystallization time, t_c. •T_c = 118° C in dodecanol, ○ T_c = 120° C in dodecanol.

The crystals from Experiment IV had a highly clustered morphology, making comparisons difficult. Close examination revealed an increasing degree of large monolayer protrusions of ill-defined shape at the periphery of the clusters as the crystallization time increased. Such morphologies are typical of those obtained from low molecular weight material and could be due to a fractionation effect. This could account for the observed thickening, and the broadening of the Raman peaks.

It should be borne in mind that the same polymer was used in all the experiments, and that fractionation effects produced no detectable change in fold length in any other case. It is possible that the effect is sufficiently more pronounced at the high temperature used in Experiment IV to cause the observed increase in fold length, but isothermal thickening may also be involved.

3.2.3. Experiment V

In an effort to eliminate the possible influence of fractionation on the results, an additional filtration was included in this experiment as explained previously. After two hours crystallization at 120.4° C, the crystal suspension was filtered, and treated in the manner described above. The filtration removes any polymer remaining in solution, thus ensuring a constant proportion of low molecular weight material in all cases. Crystal mats were prepared so that a comparison could be made between the behaviour of the same crystals in solution and in mats, to investigate the possiblity that thickening might be facilitated by increased contact between the crystals.

The uncorrected Raman data showed a shift of the LAM peaks towards lower frequencies as the crystallization time was increased. For quantitative comparisons of fold lengths a frequency correction was considered necessary in this case, since the peaks lie close to the exciting line and the possible differences in fold length are small. After background subtraction, the frequency distributions were converted to fold length distributions by applying the correction factor described by Snyder *et al.* [23]. This produced shifts of typically 1 nm in the calculated Raman fold lengths. Fig. 10 shows the results obtained. No data are available for the

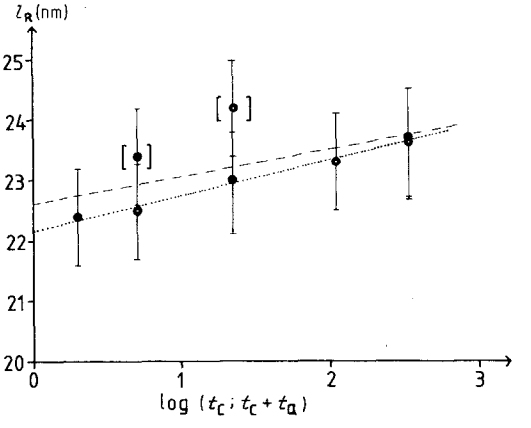

Figure 10 •Variation in Raman fold length, l_R, with crystallization time, t_c, for crystallization from dodecanol with T_c = 120.4° C. •Variation in Raman fold length, l_R, with time at T_c for the mats. The time at T_c comprises 2 h crystallization time, plus the time of subsequent annealing, t_a. The dashed line represents a least squares fit calculated from all the points. The dotted line represents a least squares fit calculated from all but the two bracketed points.

crystals from suspension with $t_c = 100$ h. A gradual broadening of the fold length distribution with crystallization time was seen. This was most apparent in the case of the crystals annealed in suspension. As in the previous experiments the results are rather inconclusive, due to the inadequate resolution of the Raman peaks and the small differences in fold length involved. However, a small increase in Raman fold length with crystallization/annealing time is indicated, and the behaviour of the crystals in suspension and in mats is similar. A least-squares fit using all the data in Fig. 10 gives a thickening rate of 0.44 nm per decade of hours. If the two spuriously high points are neglected, the rate of thickening suggested is 0.58 nm per decade.

4. Discussion

The experimental results presented here raise a number of issues which are fundamental for chain folded polymer crystallization. Let us first consider the values of T_d^0 and σ_e obtained in the various solvents. Where data are available the T_d^0 values obtained here compare well with most previous estimates [15, 25, 27]. Within the paraffin series T_d^0 would be expected to approach the melt value of 146.0° C [28] with increasing solvent chain length and this trend is indeed seen. σ_e values are rather more variable and large discrepancies occur between the various sources. Comparisons with melt data are difficult, since values for σ_e in the melt vary substantially. Measuring fold lengths by Raman spectroscopy and calculating σ_e from the fold length data in the same manner as used here gives a value of $\sigma_e = 125 \pm 12$ erg cm^{-2} for crystals grown from the melt [28]. In this work, a gradual increase in σ_e with increasing solvent chain length was seen for the paraffin series, and this too could represent a gradual transition between solution and melt crystallization. The variation of the fold length with crystallization temperature, shown in Fig. 2, follows a smooth curve for each solvent. No obvious signs of isothermal thickening are seen, although since the crystallization time was the same in all cases, small changes in fold length with time might not be apparent. When plotted as a function of supercooling the curves become to a large extent superimposed. It was mentioned in the Introduction that the kinetic theory predicts a dependence of fold length on supercooling and the verification of this dependence over a wide range of temperature, in several different solvents, lends considerable weight to the theory.

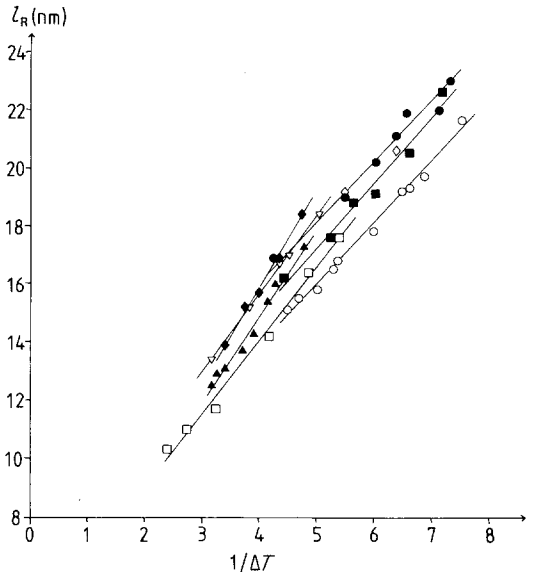

Figure 11 Raman fold lengths, l_R, plotted as a function of reciprocal supercooling, $1/\Delta T$. □-xylene, ▲-octane, ▽-dodecane, ◆-hexadecane, ○-ethyl esters, ■-hexyl acetate, ◇-tetradecanol, ●-dodecanol.

A rigorous analysis of the experimental results using the Hoffman kinetic theory requires sophisticated computer fitting of the data. However, a rough assessment can be made using the approximate equation

$$l = \frac{2T_m^0 \sigma_e}{\Delta H \Delta T} + \delta l \qquad (4)$$

where δl can be regarded as roughly constant for moderate supercoolings. Assuming σ_e and ΔH to be constant over a small temperature range, a plot of l_R against $1/\Delta T$ should yield a series of straight lines with gradients $2T_m^0 \sigma_e / \Delta H$. The results are shown in Fig. 11. In most cases the points lie on a slight curve and this curvature could be due to

TABLE II Comparison of results from kinetic theory and crystal dissolution

Solvent	$T_m^0 \sigma_e / \Delta H$ ($\times 10^{-7}$ cmK) from kinetic theory	$T_m^0 \sigma_e / \Delta H$ ($\times 10^{-7}$ cmK) from crystal dissolution
Xylene	1.25	1.23
Octane	1.51	1.34
Dodecane	1.33	1.40
Hexadecane	1.63	1.48
Hexyl acetate	1.12	1.08
Ethyl esters	1.06	1.04
Dodecanol	1.01	1.13

the neglected temperature dependence of ΔH, σ_e and δl. For comparison purposes, straight lines have been fitted to the data in Fig. 11 to give an average value of the term $T_m^0 \sigma_e / \Delta H$. These are shown in Table II together with the same quantity calculated using the σ_e values obtained from dissolution point data (see Table I) and assuming $T_m^0 = 419.2$ K and $\Delta H = 2.8 \times 10^9$ erg cm^{-3}. The results agree well in most cases, given the approximate nature of the analysis, and show Hoffman's kinetic theory to be consistent with the theory of crystal dissolution.

It would be interesting to compare the results shown in Fig. 5 with those pertaining to melt crystallized polyethylene over the same range of supercooling. Such a comparison is now possible Previous studies have given fold length values for the melt considerably higher than those from solution, but in those cases the crystals had undergone isothermal thickening during growth. The parallel work on melt crystallization in this laboratory has been aimed at identifying the unthickened fold length [2–4]. The results published so far, although taking account of what was believed to be the full extent of isothermal thickening, are nevertheless still too high to match up with those obtained here for solution. Subsequent findings regarding the true, primary unthickened fold length [5] have necessitated a revision of the melt data and as a result a complete overlap in l against ΔT dependence between melt and solution crystallization has been obtained. The full reporting of this effect [6] and the way in which the new findings on melt crystallization arose will be reported in the two additional papers to follow.

The fold length values obtained from solution are in good agreement with the predictions of the kinetic theory. However, it will be recalled that the crystal morphologies, documented in Part 1 [1], are not easily explained within this framework. A different temperature dependence is found for the habit, which is determined primarily by the crystallization temperature (in contrast to the supercooling dependence found for the fold length). Moreover, it is difficult to see how the curved crystal facets, which develop as the crystallization temperature is raised, can be made consistent with the model currently used for the kinetic theory. Having noted that the curved crystal habits arise at temperatures where isothermal thickening is known to occur in the melt, we first thought that the curvature might be a result of rearrangement of chains during isothermal thickening. Indeed the rounding of faceted habits as a result of isothermal thickening is documented in works on some special samples of melt crystallized polyethylene oxide [29]. However, the results of the ageing experiments presented here show that the rounded habits can not be explained on such a basis in our case. Certainly no thickening was detected for samples with $T_c < 118^\circ$ C, within the time scale covered by the experiments. For samples with $T_c \simeq 120^\circ$ C, a small amount of thickening was suggested, but the results were inconclusive due to the problems involved in accurate interpretation of the Raman data, and the polydisperse nature of the samples. There was no obvious difference in behaviour between crystals held in suspension at T_c and the same crystals sedimented into mats and annealed at the same T_c. The thickening, as far as its occurrence is suggested by the data, was of the order of 0.5 nm per decade, which is much lower than that observed in the melt at the same temperature.

All the samples did however show a small increase in dissolution temperature with crystallization time, and the results of gold decoration suggest that this is due to a reduction in the number of loose loops and dangling cilia on the crystal surface. This is in agreement with previous swelling results [20, 21]. Possible explanations of the effect are reorganization from loose to tight loops via reptation, although this might be expected to increase the Raman fold length, or an increase in the degree of attachment of loose chain elements to the crystal surface. The fact that Weaver and Harrison [20] found no increase in melting temperature with crystallization time is puzzling, but may be due to the much better resolution obtained in the dissolution peaks here, making small changes in peak position more obvious.

The present ageing experiments have led to some significant conclusions. Although isothermal thickening may well cause or contribute to the curving of crystal facets in the melt, the curvature of crystals obtained from solution is certainly not due to that cause and must arise in the course of the primary crystallization process. Further, it has become apparent that there is no isothermal thickening during solution crystallization at the same absolute temperatures where melt grown crystals would thicken profusely during growth. (The same statement is of course valid *a fortiori* when applied to equivalent supercoolings). Irrespective of whether the small fold length increase at the highest

temperature of 120.4° C is real or not, a basic difference between solution and melt crystallization is thus established. Confirmation that isothermal thickening does not occur during solution growth is of basic significance for the whole subject as it safeguards all previous crystal thickness measurements as being the result of primary crystallization—an assumption which has been contested [10]. This is especially important since the present framework of the kinetic theory of chain folded polymer crystallization has its roots in measurements of the primary fold lengths of solution grown crystals. To what extent the curved crystal habits are reconcilable with the models underlying the kinetic theory is another issue. A new approach to polymer crystal growth based on equilibrium surface roughness [30] may provide a better model under some conditions. One possibility is that the two approaches, while both valid in themselves, are applicable to different regimes of supercooling. The traditional nucleation based theory works well at high supercoolings, while the surface roughness based approach may be the better model at low supercoolings. The boundary between these two regimes could be defined by the T_c range which divides the morphological regimes of straight faceted and curved crystal outlines. While this would be relatively clear-cut in the case of solution growth, possible application to the melt case raises further issues. The kinetic theory has been extensively and profitably applied to melt crystallization over temperature ranges which produce curved crystal habits. Although this appears to be in contradiction with the demarcation by habit proposed above, it should be remembered that melt growth crystals have undergone extensive refolding due to isothermal thickening before observation. We do not propose to pursue this fundamental issue further here, beyond stating that according to recent results of Sadler and Gilmer [31], both classes of theory lead to the same functional l against ΔT dependence. Hence whichever pertains, and in which ΔT regime, the present fold length results from solution grown crystals and the affirmation of their origin as due to primary crystallization remains equally pertinent.

Pursuance of this discussion, while clearly invited, is beyond the scope of the present work. As already stated a separate paper, which draws together the results from melt and solution, is to follow [6]. Further experimental work designed to investigate the relationship between lateral growth rates and crystal habit is in progress.

Finally, our results show that isothermal ageing can affect the thermal stability of crystals without causing any change in fold length. This implies that the crystals, once grown, can perfect themselves, possibly at the expense of the disordered surface layer. The result is of consequence for discussions concerning the amorphous content of single crystals and the degree of disorder inherent in the fold surface. It indicates that there is no unique fold surface structure, but that whatever it is when first formed it can subsequently reorganize to produce a more perfect arrangement. It is clear from these results that the melting or dissolution points of a crystal are not necessarily uniquely associated with the fold length and hence need to be used with circumspection for fold length determination via Equation 3, a widely adopted practice.

5. Conclusions

The supercooling dependence of the fold length, as familiar from all earlier studies, has been reaffirmed over the extended T_c range here encompassed, and identified as that associated with the primary fold length by which the crystals grow. Thus the fold length seems a uniquely defined smooth function of supercooling irrespective of drastic changes in habit type, which themselves are more a function of the absolute value of the crystallization temperature. This supercooling dependence of the primary fold length is consistent with the kinetic theories of crystallization, even in the habit regime which seems presently incompatible with the model underlying these theories.

Isothermal thickening was observed to be absent (except possibly for a very small effect at the highest T_c value of 120° C) even at temperatures where the effect is prominent on melt crystallization. This finding enabled us to identify the primary fold length in crystal growth and also to associate the crystal morphologies which are seen with the primary crystallization process.

The observed increase in dissolution temperature with ageing at T_c, without an associated increase in crystal thickness, indicates that the crystals can perfect themselves with time, an effect we could attribute to regularization along the basal surface of the lamellae, hence that of the fold surface. This finding has implications for the controversial "fold surface problem", for dissolution/melting point measurements and for the interpretation of

such thermal data in terms of structural features (fold length) of the crystal.

In view of the fact that presently attained crystallization temperatures overlap with those conventionally realized on melt crystallization a correlation between these findings on solution crystallization and those of previous works on melt crystallization is clearly invited. This is undertaken in a subsequent paper [6], for which the present studies have laid the groundwork.

References

1. S. J. ORGAN and A. KELLER, *J. Mater. Sci.* **20** (1985) 1571.
2. P. J. BARHAM, R. A. CHIVERS, D. A. JARVIS, J. MARTINEZ-SALAZAR and A. KELLER, *J. Polym. Sci. Polym. Lett. Ed.* **19** (1981) 539.
3. R. A. CHIVERS, J. MARTINEZ-SALAZAR, P. J. BARHAM and A. KELLER, *ibid.* **20** (1982) 1717.
4. P. J. BARHAM, D. A. JARVIS and A. KELLER, *ibid.* **20** (1982) 1733.
5. J. MARTINEZ-SALAZAR, P. J. BARHAM and A. KELLER, *J. Mater. Sci.* **20** (1985) 1616.
6. P. J. BARHAM, R. A. CHIVERS, A. KELLER, J. MARTINEZ-SALAZAR and S. J. ORGAN, *ibid.* **20** (1985) 1625.
7. S. J. ORGAN and A. KELLER, *ibid.* **20** (1985) 1586.
8. T. KAWAI and A. KELLER, *Phil. Mag.* **11** (1965) 1165.
9. J. D. HOFFMAN, *Polymer* **24** (1983) 3.
10. J. RAULT, *J. Macromol. Sci.* **B15** (1978) 567.
11. W. O. STATTON and P. H. GEIL, *J. Appl. Polym. Sci.* **3** (1960) 357.
12. J. D. HOFFMAN and J. J. WEEKS, *J. Chem. Phys.* **42** (1965) 4301.
13. J. DLUGOSZ, G. V. FRASER, D. GRUBB, A. KELLER, J. A. ODELL and P. L. GOGGIN, *Polymer* **17** (1976) 471.
14. R. L. CORMIA, F. P. PRICE and D. TURNBULL, *J. Chem. Phys.* **37** (1962) 1333.
15. A. NAKAJIMA, F. HAMADA, S. HAYASHI and T. SUMIDA, *Kolloid Z: Z. Polym.* **222** (1968) 10.
16. A. NAKAJIMA, S. HAYASHI, T. KORENAGA and T. SUMIDA, *ibid.* **222** (1968) 124.
17. G. A. BASSETT, D. C. BLUNDELL and A. KELLER, *J. Macromol. Sci.* **B1** (1967) 161.
18. A. KELLER and D. M. SADLER, *ibid.* **B7** (1973) 263.
19. L. MANDELKERN, *J. Polym. Sci. Polym. Lett. Ed.* **5** (1967) 557.
20. T. J. WEAVER and I. R. HARRISON, *Polymer* **22** (1981) 1590.
21. Y. UDAGAWA and A. KELLER, *J. Polym. Sci. A-2* **9** (1971) 437.
22. G. V. FRASER, *Indian J. Pure and Appl. Phys.* **16** (1978) 344.
23. R. G. SNYDER, S. J. KRAUSE and J. R. SCHERER, *J. Polym. Sci. Polym. Phys. Ed.* **16** (1978) 1593.
24. R. G. SNYDER and J. R. SCHERER, *ibid.* **18** (1980) 421.
25. C. M. CORMIER and B. WUNDERLICH, *J. Polym. Sci. A-2* **4** (1966) 666.
26. J. D. HOFFMAN and J. J. WEEKS, *J. Chem. Phys.* **37** (1962) 1723.
27. T. W. HUSEBY and H. E. BAIR, *J. Appl. Phys.* **39** (1968) 4969.
28. R. A. CHIVERS, PhD thesis, Bristol University (1981).
29. A. J. KOVACS, A. GONTHIER and C. STRAUPE, *J. Polym. Sci. Polym. Symp.* **50** (1975) 283.
30. D. M. SADLER, *Polymer* **24** (1983) 1401.
31. D. M. SADLER and G. H. GILMER, *ibid.* **25** (1984) 1446.

Received 15 August
and accepted 13 September 1984